ELSEVIER

Spectrochimica Acta Part B 52 (1997) 205–218

SPECTROCHIMICA ACTA PART B

Three-dimensional density profiles of sputtered atoms and ions in a direct current glow discharge: experimental study and comparison with calculations

A. Bogaerts[a,*], E. Wagner[b], B.W. Smith[b], J.D. Winefordner[b], D. Pollmann[b], W.W. Harrison[b], R. Gijbels[a]

[a]*Department of Chemistry, University of Antwerp (UIA), Universiteitsplein 1, B-2610 Wilrijk, Belgium*
[b]*Department of Chemistry, University of Florida, Gainesville, FL 32611, USA*

Received 8 May 1996; accepted 3 August 1996

Abstract

Three-dimensional density profiles of the sputtered tantalum atoms and ions have been measured in a direct current glow discharge with flat cathode, by laser induced fluorescence spectroscopy. The primary excitation lines of the tantalum atoms and ions are taken to be the 269.131 nm and the 270.280 nm lines, respectively, whereas the 358.42 nm line and the 304.2 nm line are used as their fluorescence lines, respectively. Moreover, atomic absorption measurements with a hollow cathode lamp were also performed to check the fluorescence results for the atoms. The 271.467 nm line was selected for this purpose. The discharge was studied for a range of voltages, pressures and currents (i.e. 700–1200 V, 0.7–1.6 torr, 1.2–3.9 mA). The atom density profile reaches a maximum at about 3 mm from the cathode, whereas the ion density profile was found to be at its maximum at about 6 mm from the cathode. The experimental data have been compared with results of mathematical simulations for the same geometry; in general, satisfactory agreement is reached. Experimental observations and modeling calculations allow better insight into the complex interactions occurring in a glow discharge.

Keywords: Direct current glow discharge; Glow discharge diagnostics; Three-dimensional profiles; Sputtering; Tantalum; Laser induced fluorescence; Discharge modeling

1. Introduction

During the last few decades, glow discharges are finding increased application as atomization/excitation/ionization sources in analytical chemistry [1–3]. To improve the analytical results, a better insight into glow discharge processes is desirable. This can be obtained by mathematical modeling and by experimental plasma diagnostics. In analytical glow discharges, special interest exists for the behavior of the sputtered atoms. Therefore, attention is given to these species in the present paper. A mathematical model for the description of the sputtered atoms and corresponding ions was developed by Bogaerts and Gijbels in one dimension [4] and in three dimensions [5]. This model fits into a more complex network of models describing the most important species in the glow discharge (electrons, argon atoms and ions, argon metastable atoms, and sputtered atoms and ions) [6–12]. However, to test the validity of the models, the theoretical results have to be compared with experimental data. Sputtered atom density

* Corresponding author.

0584-8547/97/$17.00
PII S0584-8547(96)01577-7

profiles in a glow discharge have been measured by many authors. In Refs. [13–15] relative number density profiles were obtained by atomic absorption and in Ref. [16] by atomic fluorescence. Also, absolute number density profiles have been presented in literature, resulting from atomic absorption measurements [17–19] and from the COMAS (Concentration-Modulated Absorption Spectroscopy) technique [20,21]. These density profiles are, however, mostly one-dimensional, i.e. as a function of axial position from the cathode. To our knowledge, measurements of the sputtered species ion densities have not yet been reported in literature.

In this paper, we present complete three-dimensional absolute density profiles of the sputtered atoms and corresponding ions, obtained by laser fluorescence measurements. Moreover, the absolute sputtered atom density is also measured by atomic absorption to verify the experiments. Tantalum was chosen as sputtered species, since it has atom and ion lines lying close enough together to be used with the same dye laser.

2. Theoretical background

2.1. Fluorescence measurements

Fluorescence measurements yield a three-dimensional fluorescence intensity profile. From this fluorescence intensity, it is possible to calculate the absolute number density. A part of the energy level scheme of the Ta atoms and ions is illustrated in Figs. 1(a) and 1(b) respectively, together with the relevant wavelengths and corresponding transition probability values of the laser excitation and of the fluorescence pathways. These transition probability values were obtained from Corliss and Bozman [22]. However, since these values are subject to uncertainties, they were only used as branching ratios (i.e. relative values). The absolute values were obtained by measuring the lifetime of level 3 by fluorescence. It was ascertained that there was no collisional quenching in the glow discharge, so that the lifetime of level 3 is only determined by the radiational transitions given in Figs. 1(a) and 1(b). The lifetime of the excited Ta atoms was measured to be 33.3 ns; the lifetime of the excited Ta ions was 12.9 ns. We found no

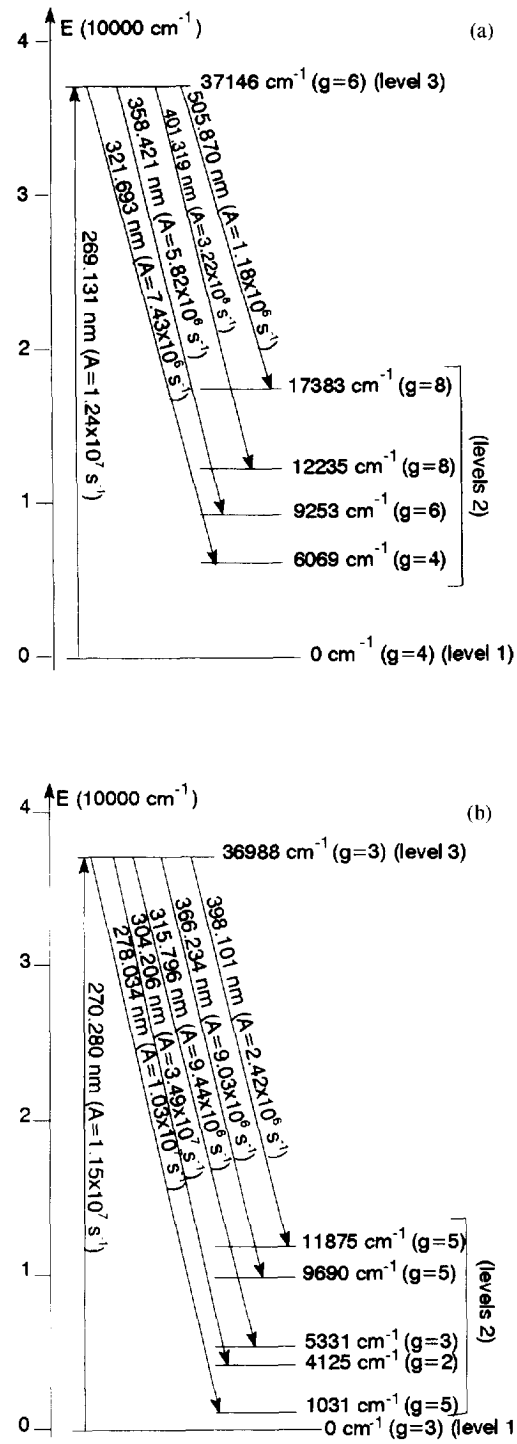

Fig. 1. Part of the energy level scheme and relevant excitation and fluorescence lines for the Ta atoms (a) and Ta ions (b); g is the level degeneracy, A is the transition probability.

literature value for the lifetime of the excited Ta atoms, but the lifetime obtained for the excited Ta ions is in excellent agreement with Ref. [23] where a value of 12.2 ns was reported.

The laser excites the species from the ground state level (level 1) to level 3, which can relax by fluorescence to the levels 2. In the experiments, we selected the 358.42 nm wavelength for the Ta atoms, and the 304.2 nm wavelength for the Ta ions, since both fluorescence lines have a high transition probability. From the fluorescence intensity, the absolute number density of level 3 can be derived, and from the number density of this level, the total number density of Ta atoms and ions can be calculated. Since the experiment was performed with a short pulsed laser (see below), the level populations do not reach a steady state value. Therefore, the measured fluorescence intensity yields the number density of level 3 integrated over time [24]

$$B_F = h\nu_{32}\left(\frac{\ell}{4\pi}\right)A_{32}\int n_3\,dt$$

where B_F is the fluorescence intensity resulting from a single laser pulse (J cm^{-2}sr^{-1}), h is Planck's constant (J s), ν_{32} is the frequency of the fluorescence line (s^{-1}), ℓ is the path length in which fluorescence takes place (defined by the laser beam diameter; i.e. 0.05 cm), A_{32} is the Einstein transition probability of the fluorescence transition (i.e. 5.82 × 10^6 s^{-1}) and n_3 is the number density (cm^{-3}) of level 3, which is integrated over time from one laser pulse to the next.

In order to relate n_3 to the total number density of Ta atoms and ions, a software program based on a density matrix model (DENSMAT) [25,26] was used. This program calculates the relative level populations as a function of time, when the laser irradiance, the laser bandwidth, the laser pulse temporal profile, the rate constants of different relaxation pathways and the level degeneracies are given. Figs. 2(a) and 2(b) show the results of the DENSMAT calculations for the Ta atoms and ions, respectively. The laser pulse has a duration of about 2.5 ns and the laser repetition rate is 9 kHz (i.e. about 0.1 ms between two pulses). As a result of the laser pulse, the population of level 1 initially shows a sharp drop, whereas the population of level 3 increases. After a few nanoseconds, the population of level 3 decreases again as a result of relaxation to the levels 2. Consequently, the

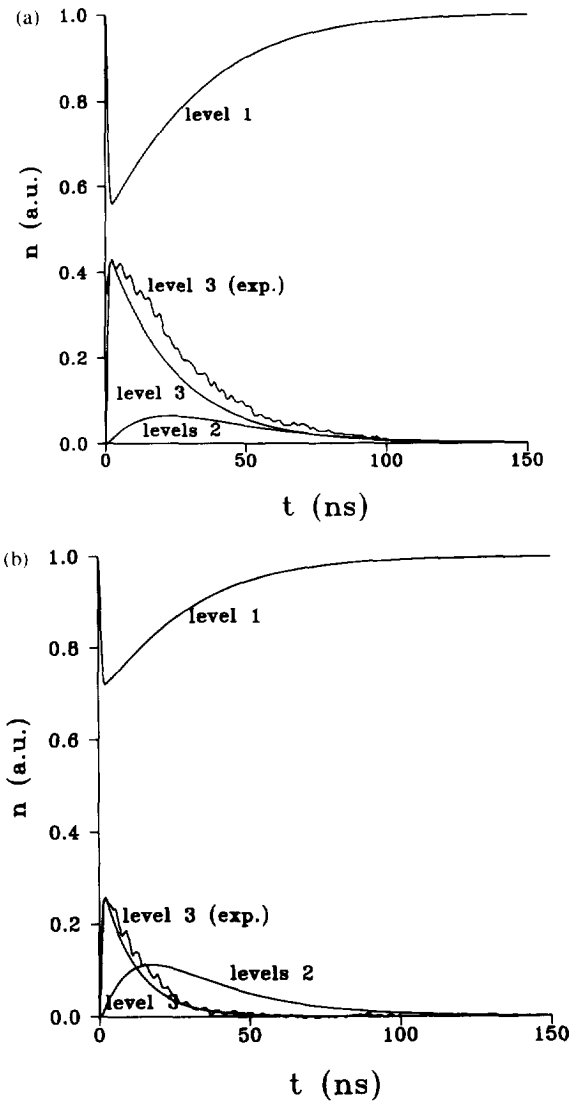

Fig. 2. Relative population time profiles of levels 1, 2 and 3, calculated with the DENSMAT program, and comparison with the experimental time profile of level 3 obtained with fluorescence, for the Ta atoms (a) and the Ta ions (b).

population of the levels 2 starts to rise. The relaxation rate from levels 2 to level 1 was assumed to be 4 × 10^7 s^{-1}. It follows then that the levels 2 relax to the ground state after a few 100 ns, and the level 1 population returns again to its initial value of 1. The uncertainties in the assumed relaxation rate from levels 2 to level 1 may be reflected in the number densities calculated. For comparison, the experimentally obtained time profiles of level 3 for the Ta atoms and ions,

derived from the fluorescence temporal profiles are also presented, with their intensities scaled to the calculated profiles. It can be seen that a reasonably good agreement is reached between the experimental and the calculated profiles.

The temporal profiles of the level populations calculated by DENSMAT are on a relative scale, i.e. the total number density of Ta atoms and ions is equal to 1. By dividing the time integrated absolute population density calculated from the fluorescence intensity (see above) by the relative temporal profile of level 3 calculated from DENSMAT, the absolute number densities of the Ta atoms and ions can finally be obtained.

2.2. Absorption measurements

To test the reliability of the above fluorescence density measurements, absorption measurements were also performed, i.e. the fluorescence measurements served now only to yield the relative density profile, and the absorption measurements were carried out to put an absolute number on this profile. The absorption measurements yield an integrated absorbance signal at a certain axial position (side-on measurements, integrated over the total radial distance), which can be converted to a density integrated over the total radial distance (see below), i.e. the sum of all irradiated radial positions at that axial position. This integrated density (summed over the total radial distance) is related to the sum of the fluorescence intensities for all radial positions at that axial position, and the fluorescence intensities at each individual radial position then yield the absolute number densities at all the different radial positions.

It was not possible to use the laser for the absorption measurements, since the laser bandwidth (ca. 10 pm) was much larger than the absorption profile (i.e. ca. 0.35 pm) and absorption could barely be detected. Therefore, a Ta–Ne hollow cathode lamp (HCL) was used. The absorption measurements were only performed for the Ta atoms, since the Ta ion lines emitted by the HCL were either too weak or could not sufficiently be distinguished from other lines to permit reliable measurements. For the Ta atom measurements, the 271.467 nm line was selected.

The absorbance curve for this line was first calculated for a range of densities. Since the emission line width of the excitation source (HCL) and the absorption line width of Ta atoms in the glow discharge are of comparable magnitude, the approximations usually made for a line source or a continuum source [27] cannot be carried out, and the complete formula has to be used [28,29]

$$A = \log \frac{I_i}{I_t}$$

$$I_i = \int I_0 f(\nu)\, \mathrm{d}\nu$$

$$I_t = \int [I_0 \exp(-k_0 g(\nu)\ell)] f(\nu)\, \mathrm{d}\nu$$

where A is the absorbance, I_i is the total incident line intensity, I_t is the total transmitted line intensity, I_0 is the incident line intensity at the maximum of its profile, $f(\nu)$ is the line profile of the source line, k_0 is the absorption coefficient, $g(\nu)$ is the line profile of the absorption line and ℓ is the absorption path length. The line profile of the source line (emission line of the HCL) is almost entirely determined by Doppler broadening [30]

$$f(\nu) = \exp\left[-\left(\frac{2(\nu - \nu_0)\sqrt{\ln 2}}{\Delta\nu_D} \right)^2 \right]$$

where

$$\Delta\nu_D = \frac{2\sqrt{\ln 2}}{c} \nu_0 \sqrt{\frac{2RT}{M}}$$

Since a HCL and a conventional glow discharge emit lines with comparable profiles, the absorption line profile, $g(\nu)$, can be taken equal to $f(\nu)$. This yields for the absorbance formula

$$A = \log \frac{I_i}{I_t} = \log \left(\frac{\int I_0 f(\nu)\, \mathrm{d}\nu}{\int I_0 f(\nu) \exp(-k_0 f(\nu)\ell)\, \mathrm{d}\nu} \right)$$

The absorption coefficient k_0 correlates to the number density N by [27,31]

$$k_0 = \frac{\sqrt{4\pi \ln 2} e^2 \lambda_0^2 N f}{m c^2 \Delta\lambda_D}$$

where e and m are the electronic charge and mass, c is the speed of light, λ_0 is the wavelength at the center of

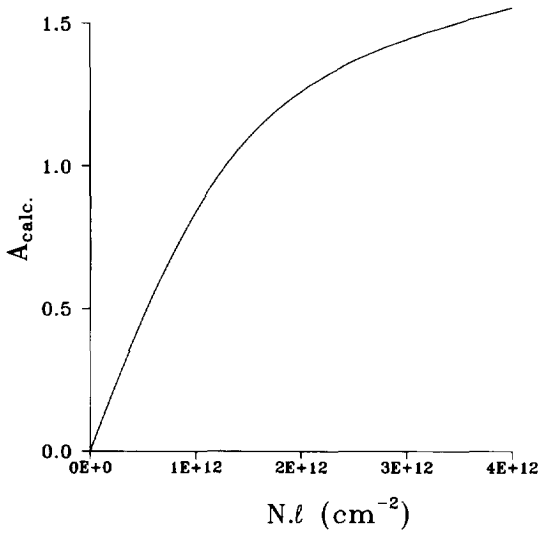

Fig. 3. Calculated absorbance curve for the Ta atoms; ℓ is the optical path length in cm and N the atom density per cm^3.

the profile, $\Delta\lambda_D$ correlates to $\Delta\nu_D$ (see above), and f is the oscillator strength of the absorption transition. Hence, these formulas are used to calculate the absorbance for a range of densities, resulting in an absorbance curve (see Fig. 3). By comparing the measured absorbances with the calculated absorbance curve, the absolute (integrated) number densities can be obtained, from which the individual number densities at each position can be derived (explained above).

3. Experimental setup

For the fluorescence measurements, a copper vapor laser (Model CU15-A, Oxford Lasers, Acton, MA) was used to pump a dye laser (Model DLII, Molectron) at a repetition frequency of 9 kHz. The dye laser (Rhodamine 560, Exciton Corp., Dayton, OH) output was frequency doubled in a KDP "R6G" crystal and the fundamental frequency filtered to obtain the 269.131 nm Ta atom excitation line and the 270.28 nm Ta ion excitation line which were typically 1 μJ in a pulse duration of 2.5 ns (FWHM). The spectral irradiance necessary to saturate these transition lines was not reached. The beam was gently focused into the glow discharge chamber by a 25.4 cm focal length fused silica lens. The emitted fluorescence was collected at 90° from the excitation beam path and imaged onto the monochromator (Minimate Model, 1200 g mm^{-1} grating, Spex, Edison, NJ) entrance slit by a 5 cm dia. biconvex fused silica lens, reduced by an aperture to a diameter of 2 cm to provide f/10 collection. The slit width was 250 μm and the height was masked to 1 mm to match the laser beam geometry and to provide good spatial resolution. The signal was detected with a PMT (R955, Hamamatsu Corp., Bridgewater, NJ) conditioned with transimpedance amplifier (Model A1, Thorn EMI Gencom, Inc., New York) and processed with a boxcar integrator (SR250, Stanford Research, Sunnyvale, CA) interfaced to a personal computer.

For the absorption measurements, a Ta–Ne hollow cathode lamp (Fisher Scientific, Pittsburgh, PA) operating at 20 mA was used. The transmitted light was imaged on the entrance slit of another monochromator (GCA McPherson Instruments) with better spectral resolution in order to make sure that the Ta 271.467 nm line was clearly resolved.

The glow discharge chamber was a stainless steel six-way cross with 4 cm dia. ports. Four ports, lying in the same plane, are provided with quartz windows and are used for the absorption and fluorescence measurements. The 5th port goes to the vacuum pump and the 6th has a fitting which permits the insertion of the cathode probe. The glow discharge chamber is mounted on a table which can be moved in the x, y and z directions, in order to carry out three-dimensional spatially resolved measurements. Measuring points were taken at 1 mm intervals from the cathode (until 8 mm from the cathode), and at each 2 mm further away from the cathode. It was tested that different x–y combinations which corresponded to the same radial distance from the cell axis, yielded the same fluorescence signal. This demonstrates the approximate cylindrical symmetry of the discharge cell, and it shows that the incoming laser light and outgoing fluorescence light are not further absorbed in the glow discharge plasma.

The entire glow discharge chamber is grounded and acts as anode; the cathode is at high voltage. Tantalum disks of about 1 mm thick, obtained by cutting from a tantalum rod (99.99% pure, 4.5 mm in diameter; Alfa Aesar, Ward Hill, MA), were used as cathode. The disks were glued onto the cathode insertion probe using silver impregnated paint. A Teflon® shield was placed around the tip of the probe and the edge

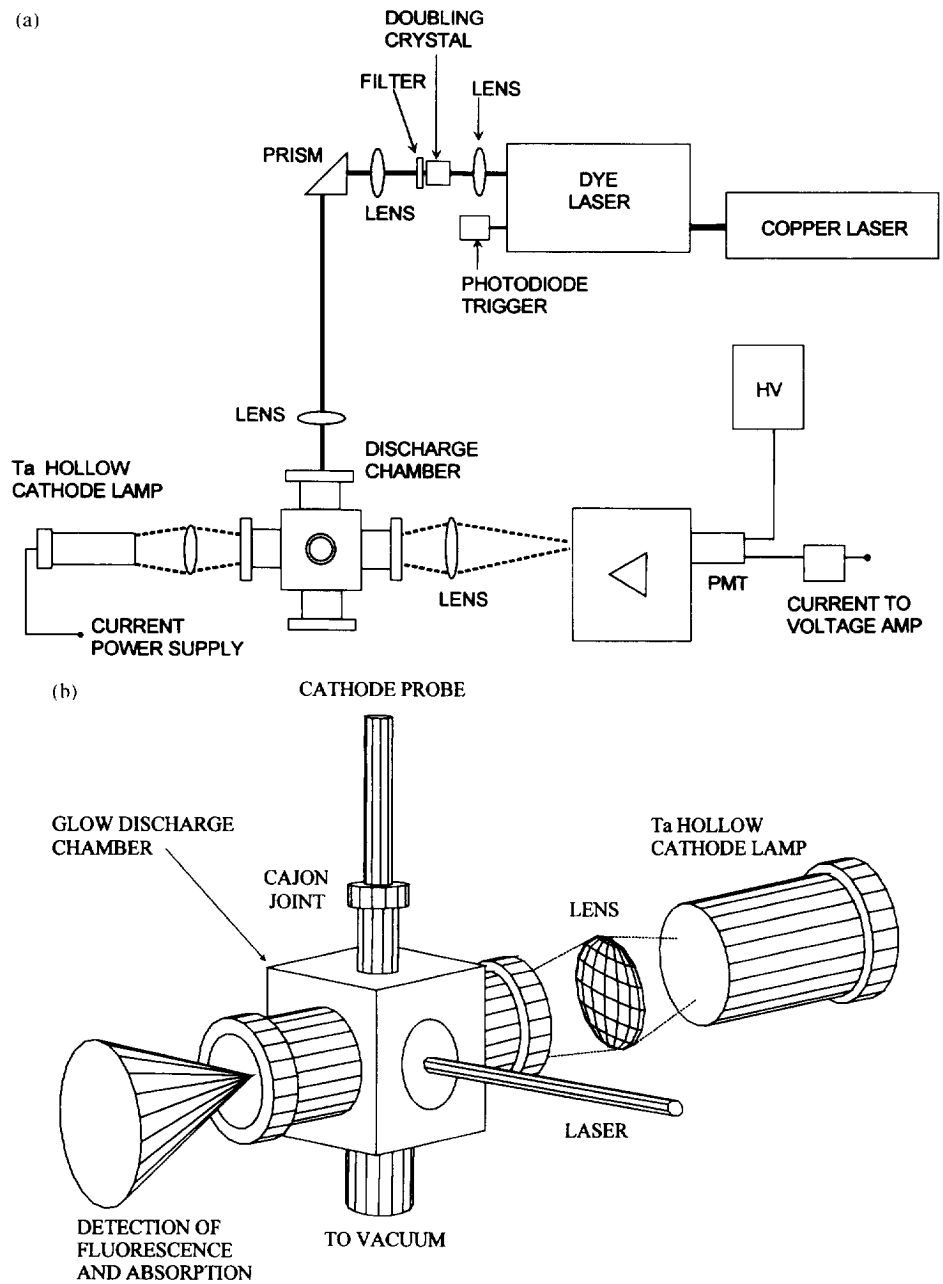

Fig. 4. Schematic overview of the experimental setup (a) and of the glow discharge geometry (b).

of the sample disk so that only the Ta sample was exposed to the discharge. A schematic overview of the experimental setup and of the glow discharge in detail are given in Figs. 4(a) and 4(b), respectively.

The output signal from the fluorescence measurements at the computer is given in volt. To calculate the level population, the fluorescence intensity must be expressed in J $cm^{-2}sr^{-1}$. The conversion of this fluorescence intensity was accomplished in the following way: B_F (J $cm^{-2}sr^{-1}$) was the output signal (V), divided by (i) the gain of the electronics (preamplifier and boxcar; k_1 in V $A^{-1}s^{-1}$), (ii) the response

of the monochromator and PMT (k_2 in A W^{-1}), (iii) the slit area of the monochromator (i.e. 250 μm × 1 mm = 0.0025 cm^2), (iv) the solid angle of the system (calculated to be 0.00784 sr) and (v) the transmission of the windows (measured to be 0.865) and lenses (0.92 when assuming 4% surface losses at each side). To achieve accurate values of k_1 and k_2, the electronics, the monochromator and the PMT had to be calibrated. The gain of the electronics was obtained by measuring the fluorescence peak directly with an oscilloscope (in A s) and correlating it with the fluorescence signal after passage through the preamplifier and boxcar (in V). This yielded a k_1 value equal to 1.11×10^{11} V $A^{-1}s^{-1}$. The monochromator and PMT were calibrated with a He–Cd laser (Liconics, Sunnyvale, CA) of 0.94 mW at 325 nm, imaged with the same optics as used for the fluorescence measurements. The power behind the entrance slit of the monochromator was measured with a calibrated photodiode (United Detector Technologies, PIN-10DP). The photocurrent reaching the PMT, corresponding to this amount of radiation, was measured at the different PMT voltages used for the experiments. Dividing this measured photocurrent by the measured power behind the entrance slit, yielded the response of the monochromator and PMT at 325 nm. The response at the fluorescence wavelengths (358.42 nm and 304.206 nm) was obtained by using a 1000 W quartz–halogen tungsten-coiled coil-filament lamp, which served as a standard of spectral irradiance (Model FEL-C). The resultant k_2 for a PMT voltage of 1000 V at 358 nm and 304 nm was found to be ca. 76 300 and 56 560 A W^{-1}, respectively.

4. Mathematical model

A mathematical model for the sputtered atoms and ions was developed earlier in one dimension [4] and later for the three-dimensional geometry of the standard cell for analyzing flat samples in the VG9000 glow discharge mass spectrometer [5]. The atoms are sputtered from the cathode and lose their initial energies of a few eV almost immediately by collisions with gas particles (thermalization process). When they are thermalized, further transport is diffusion dominated. The sputtered atoms can be ionized by Penning ionization, asymmetric charge transfer and electron impact ionizaton. The transport of the ions created in this way is controlled by diffusion and migration. More details about the physics and mathematics of the models can be found in the above cited papers. In order to compare the experimental and modeling results, the complete three-dimensional model network [5,11] was modified and applied to the experimental cell geometry. More correctly, the experimental cell geometry (six-way cross) was approximated by a cylinder of 4 cm dia. and 2 cm length, and a Ta cathode of 4.5 mm dia. The secondary electron emission coefficient of Ta is taken as 0.11 [32]. A sticking coefficient of 0.5 for Ta and 1.0 for Ta^+ is assumed.

5. Results and discussion

Fig. 5 shows the three-dimensional Ta atom density profile at 1000 V, 1 torr and 2 mA, obtained by the fluorescence measurements. Due to the cylindrical

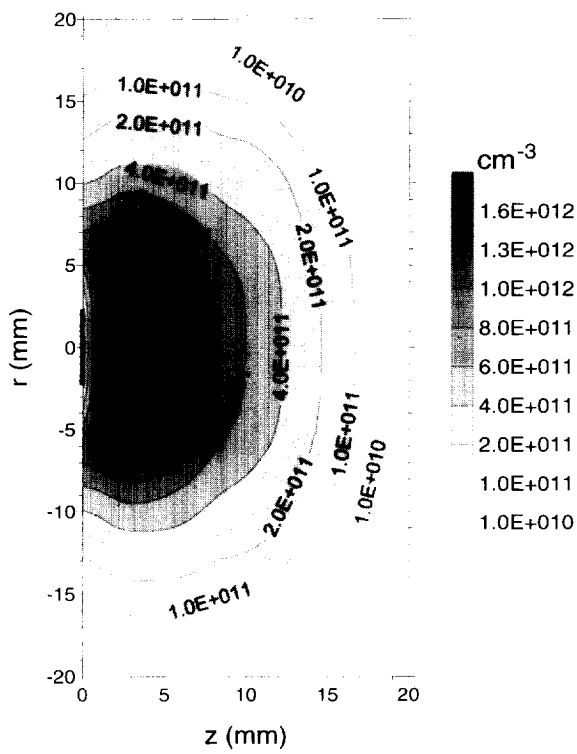

Fig. 5. Experimental density profile of the Ta atoms, obtained by laser induced fluorescence, in an argon glow discharge at 1000 V, 1 torr, 2 mA.

geometry of the discharge plasma, the three-dimensional profile can be presented in two dimensions. The position of the cathode is indicated with the black line at the z and r equal to zero. The density is low close to the cathode, it increases and reaches a maximum at about 3 mm from the cathode whereafter it decreases gradually towards the cell walls. The cathode (0–0 point) is located at the center of the cell. Since the cell windows were only 20 mm in radius, we could only detect fluorescence intensity within 20 mm from the 0–0 point. The fact that the sputtered atom density shows a dip in front of the cathode was also found in other papers [13,15,18]. It was explained by assuming that not all the cathode material is sputtered as neutral atoms, but that a certain amount is maybe released as clusters or excited state species, which are not detected by atomic absorption or fluorescence. This explanation sounds quite reasonable. However, a similar profile also results from our modeling calculations (see below),

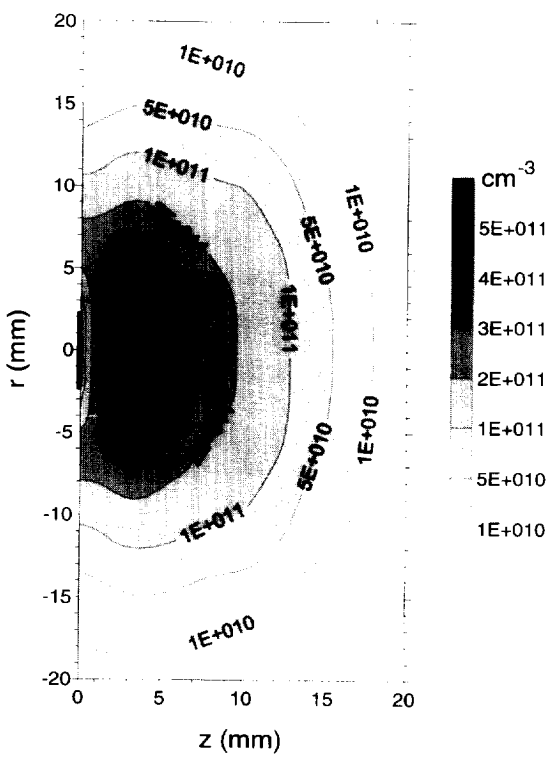

Fig. 6. Experimental density profile of the Ta atoms, obtained by combined fluorescence and absorption, in an argon glow discharge at 1000 V, 1 torr, 2 mA.

without taking into account sputtering in the form of clusters. Indeed, the sputtered atoms leave the cathode with energies of several eV. They lose these initial energies very rapidly by collisions with argon gas atoms, until they are thermalized. This gives rise to a thermalization profile (i.e. the number of sputtered atoms thermalized as a function of position from the cathode), which shows a maximum at about 1 mm from the cathode (see Refs. [5,7]). Since thermalization is much faster than diffusion, thermalization is already finished when diffusion starts, and the thermalization profile serves as starting distribution for the diffusion away from the cathode and back to the cathode. This explains why the sputtered atom population is at maximum at a few mm away from the cathode. Indeed, a model where such an initial thermalization step is not included (e.g. Ref. [18]) cannot predict the dip in front of the cathode. Fig. 6 shows the three-dimensional Ta atom density profile at the same discharge conditions, obtained by atomic absorption. The relative profile is the same, since it results from the same fluorescence measurements. The absolute value of the atom densities is a factor of 3 lower than for the fluorescence experiment. This illustrates the magnitude of the relative errors encountered in these experiments.

In Fig. 7, the Ta atom density profile, resulting from the modeling calculations at 1000 V, 1 torr and 2 mA, is presented. Comparison of Figs 5–7 shows that the relative profiles of experiment and theory are very similar. A maximum is also reached at a few mm from the cathode. Only at $z = 0$, are the modeling results slightly different. This is explained by the fact that for simplicity a cell wall was assumed at $z = 0$ in the model, whereas in reality an insertion probe is used as cathode and the glow discharge chamber also extends to negative z-values for $r >$ 2.25 mm. The absolute value at the maximum of the calculated density profile is a factor of 2 higher than the fluorescence result and a factor of 6 higher than the absorption result. However, at distances further into the discharge, the calculated result lies in between the fluorescence and the absorption result. Indeed, the atom density from the modeling seems to drop somewhat more rapidly from the maximum than the experimental results. Taking into account the experimental errors (see for example the difference between fluorescence and absorption results) and the

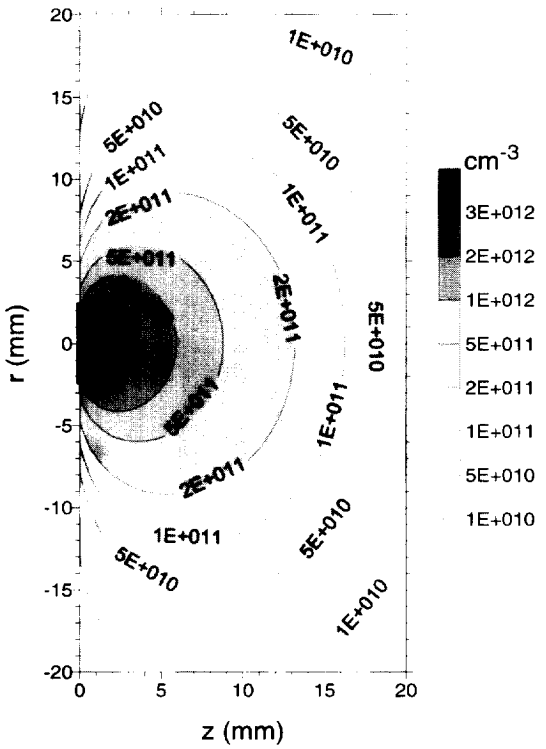

Fig. 7. Density profile of the Ta atoms, obtained by modeling calculations, in an argon glow discharge at 1000 V, 1 torr, 2 mA.

approximations of the model, it can be concluded that an excellent agreement is reached between experiment and theory.

The densities reported in the literature for sputtered atoms are generally higher than the values obtained in this work, i.e. about $1-5 \times 10^{13}$ cm^{-3} for a hollow cathode lamp [17,19] and for a Grimm-type glow discharge [18]. However, both the hollow cathode lamp and the Grimm type glow discharge operate at much higher currents so that higher sputtered atom densities are indeed expected. The results obtained with the COMAS technique [20,21], on the other hand, are lower than our results, i.e. about 10^{11} cm^{-3} for a hollow cathode lamp, and about $10^{9} - 10^{10}$ cm^{-3} for a plane parallel glow discharge.

To investigate the influence of voltage, pressure and current on the density profiles, the experiments were performed for a range of discharge conditions. Figs 8(a) and 8(b) show the one-dimensional density profiles at the cell axis at constant pressure for 4 different voltage and current values, obtained by fluorescence and absorption, respectively. Analogously,

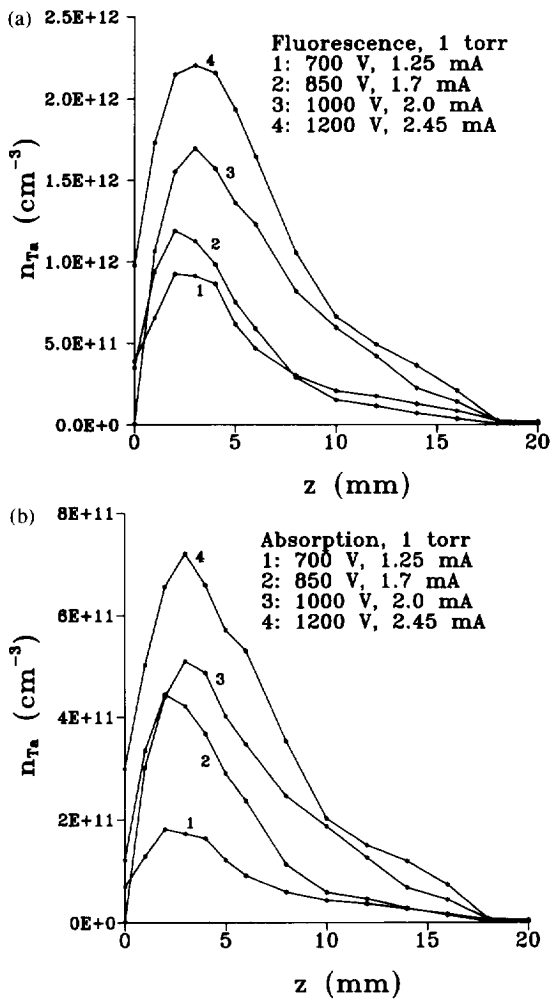

Fig. 8. One-dimensional density profiles of the Ta atoms along the cell axis, at 1 torr for a range of different voltages, obtained by fluorescence (a) and by absorption (b).

Figs 9(a) and 9(b) present the one-dimensional density profiles for 4 different pressures and currents at constant voltage, by fluorescence and absorption, respectively. The shapes of the profiles do not appear to be influenced by the discharge conditions. However, the absolute values of the densities clearly increase with increasing voltage, pressure and current. Indeed, at higher pressures and currents, there is a higher flux of plasma species bombarding the cathode, leading to more sputtering and hence a higher sputtered atom population. At higher voltages, the energy of the bombarding plasma species is higher, which also results in more sputtering.

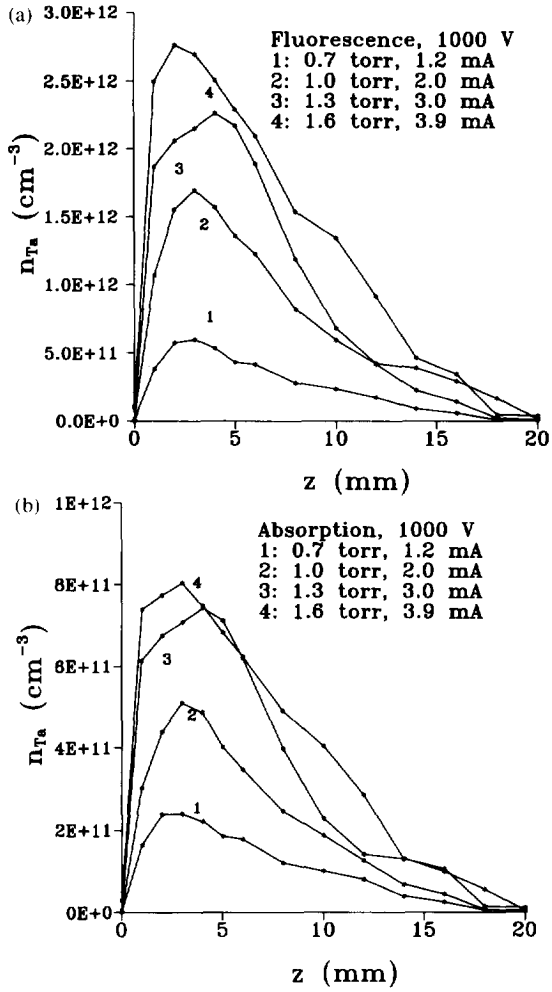

Fig. 9. One-dimensional density profiles of the Ta atoms along the cell axis, at 1000 V for a range of different pressures, obtained by fluorescence (a) and by absorption (b).

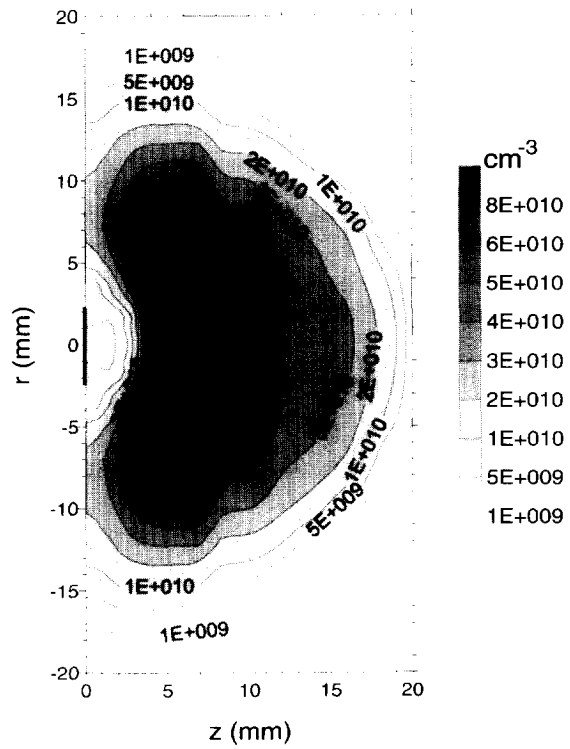

Fig. 10. Experimental density profile of the Ta ions, obtained by laser induced fluorescence, in an argon glow discharge at 1000 V, 1 torr, 2 mA.

Fig. 10 shows the three-dimensional density profile of the Ta ions at 1000 V, 1 torr and 2 mA, obtained by fluorescence measurements. The Ta^+ number density is low and rather constant in the cathode dark space, increases to a maximum at about 6 mm from the cathode, and decreases also towards the cell walls. The maximum number density is reached at greater distances from the cathode than for the Ta atoms. The experimental number density profile shows excellent qualitative agreement with the result of the modeling calculations for the same discharge conditions, presented in Fig. 11. Indeed, the number density is low in the cathode dark space (the fact that it is slightly different near the cathode is again due to the approximations of the geometry in the model) and it reaches also a maximum at about 5–6 mm from the cathode. However, the absolute value at the maximum in the modeling result is almost a factor of 10 lower than the experimental result, which is a result of calculation values being too low or experimental results being too high. In the model, the Ta ion density is calculated from the Ta atom density taking into account three ionization processes: electron impact ionization, Penning ionization and asymmetric charge transfer. Since the Ta atom density is in good agreement with experiment, it suggests that the amount of ionization in the calculations is too low. There are several possibilities: either one of the above mentioned ionization mechanisms is underestimated or there are still other ionization pathways which are not incorporated in the model. The amount of electron impact ionization is determined by the electron flux and the cross section of electron impact ionization. Since the calculated electron flux is directly related to the calculated total

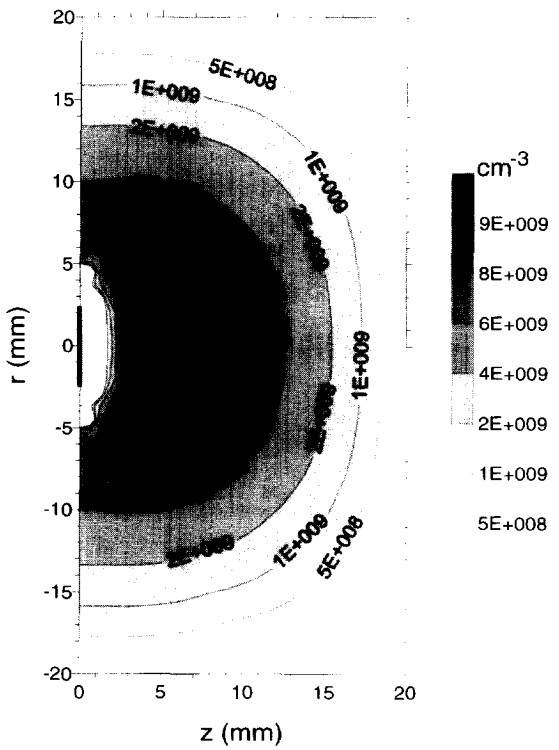

Fig. 11. Density profile of the Ta ions, obtained by modeling calculations, in an argon glow discharge at 1000 V, 1 torr, 2 mA.

electrical current, and since the latter one is in perfect agreement with experiment (i.e. 2 mA), we think that the electron flux is correct. The cross section of electron impact ionization was derived from a formula in Ref. [33], and in general this value is rather well known in the literature for different elements. Therefore, the amount of electron impact ionization is assumed to be calculated correctly. The amount of Penning ionization is given by the argon metastable atom density and the rate constant of Penning ionization. The calculated argon metastable atom density has been compared with experiment [34] and the absolute values showed satisfactory agreement. Close to the cathode, the modeling results were even too high compared with experiment, so that it is not very likely that the calculated argon metastable atom density is underestimated. The rate constant of Penning ionization was calculated from a formula in Ref. [35] to be 2.76×10^{-10} cm^3 s^{-1}. A value of the order of 10^{-10} cm^3 s^{-1} is indeed generally cited in the literature for Penning ionization of different elements. Hence, the amount of Penning ionization is also expected to be calculated more or less correctly. The extent of asymmetric charge transfer depends on the argon ion density and the rate constant of this process. The argon ion density is also related to the total electrical current and its value is therefore assumed to be also correct. The rate constant of asymmetric charge transfer between Ar ions and Ta atoms could not be found in the literature. In previous work [9], this rate constant was taken to be equal to the Penning ionization rate constant if the element possessed ionic energy levels suitable for asymmetric charge transfer (i.e. lying close to the argon ion energy levels). An extensive study about the availability of such levels for most elements of the periodic table was made in Ref. [36]. Ta was not included in this study, since the Ta ion energy level scheme in the literature [37] is incomplete (i.e. the energy levels lying in the region of interest are not recorded in Ref. [37]). However, based on the periodic table, Ta belongs to the group of elements which possess many levels for asymmetric charge transfer, therefore it is assumed that the rate constant of asymmetric charge transfer between Ar ions and Ta atoms is equal to the Penning ionization rate constant. Based on this assumption, it was calculated that the relative contributions of electron impact ionization, Penning ionization and asymmetric charge transfer at 1000 V, 1 torr and 2 mA amount to about 1, 8 and 91%, respectively. Hence, asymmetric charge transfer is calculated to be clearly dominant. Although in earlier reviews of GDMS, it has often been stated that Penning ionization is the dominant process and that asymmetric charge transfer only plays a secondary role, some other papers demonstrate that this process is very important in a glow discharge for certain ion–atom combinations [38–46]. Due to the uncertainties in the rate constant, we have to be cautious about the role of asymmetric charge transfer. However, the fact that the calculated Ta ion density is too low compared to experiment, could indicate that this process is indeed important and may still be underestimated. Indeed, in Ref. [19], a rate constant of 10^{-9} cm^3 s^{-1} was used between Ne ions and Cu atoms. Using such a high rate constant would indeed give good agreement between the calculated and experimental Ta ion density. An alternative explanation for the discrepancy between experiment and theory would be that other ionization pathways

are important which are now neglected in the model, like photoionization, ion or atom impact ionizaton, or dissociative ionization involving clusters of Ta. The latter assumption is not too unreasonable, since Ta has a high affinity for oxygen. It may be possible that TaO molecules are dissociated and ionized into Ta^+ upon impact by electrons or other plasma species. However, since the necessary data to prove this (i.e. TaO number density in the plasma, cross sections of possible alternative ionization processes) are not available, this explanation remains only speculative. On the other hand, it is also possible that the difference between experiment and theory is due to the fact that the experimental results are too high. It is difficult to estimate the experimental uncertainties. From Figs 5 and 6, it was deduced that the error can be at least a factor of 3 (and it may be more if the good agreement between the fluorescence and absorption data would only be coincidence). It is very reasonable to believe that the discrepancy between Figs 10 and 11 is a combination of some limitations in the model and some experimental errors. After all, a factor of 10 difference between experiment and theory is not too bad, when we consider that neither such experiments nor such modeling calculations have ever been performed and compared before.

The influence of voltage, pressure and current on the one-dimensional Ta ion density profile is illustrated in Figs 12(a) and 12(b). In analogy to the Ta atom density, the absolute value of the Ta ion density clearly increases with voltage, pressure and current, but the shape of the profile remains rather unaffected.

Finally, from the ratio of the Ta ion density to the Ta atom density, the ionization degree of Ta can be deduced. Experimentally, a value of about 5% is obtained, whereas the modeling calculations predict a value of 1.7%. Hence, although the absolute values of the number densities are not yet in complete agreement between experiment and theory, the ratio of atom and ion densities is in satisfactory agreement. These values are slightly higher than general statements ("1% or less") in GDMS literature [1,2]. This could be attributed to the fact that we measure only ground state Ta atom and ion populations. When a considerable fraction of the Ta atoms is in a metastable excited state, they are not detected by the fluorescence. The experimentally obtained ionization

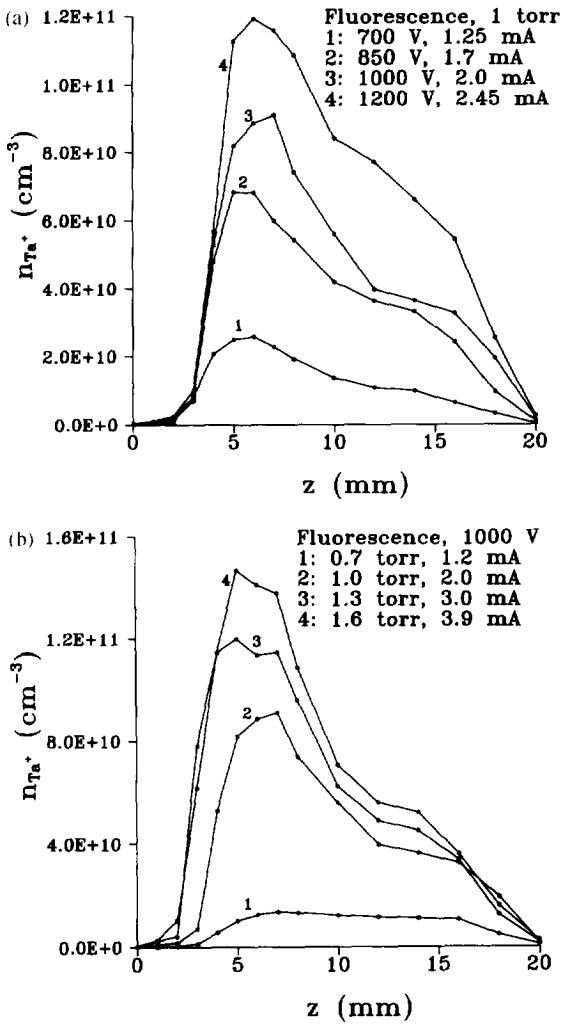

Fig. 12. One-dimensional density profiles of the Ta ions along the cell axis, in an argon glow discharge at 1 torr for a range of different voltages (a), and at 1000 V, for a range of different pressures (b).

degree would then be an upper value. However, it is expected that the number of Ta atoms in the excited states is negligible to the number of ground state atoms, so that the effect will probably be unimportant. In any case, it would be dangerous to generalize the obtained value of the ionization degree, since it depends on specific atom–ion combinations (especially asymmetric charge transfer), on the discharge conditions and on the cell geometry (i.e. in the cell of the VG9000 mass spectrometer, the same mathematical model yields values of 0.1% and less for Cu [5]).

6. Conclusion

Three-dimensional number density profiles of sputtered Ta atoms and Ta ions have been measured in a glow discharge by atomic fluorescence and absorption. The Ta atom number density reaches a maximum at about 3 mm from the cathode and decreases gradually towards the cell walls. The results of the fluorescence and absorption measurements differ by a factor of 3, which illustrates the magnitude of the errors that can be expected for the present results. The Ta ion number density is low and rather constant in the cathode dark space and reaches a maximum in the center of the negative glow at about 5–6 mm from the cathode. The influence of voltage, pressure and current on the densities is investigated and it is found that both the atom and ion number densities increase with voltage, pressure and current. The experimental number density profiles have been compared with results of modeling calculations, and reasonable agreement is reached. The combination of both these experiments and the mathematical modeling has never been done before. Therefore, although perfect agreement has not yet been obtained, the results certainly give a better understanding of the glow discharge.

Acknowledgements

A. Bogaerts is indebted to the Belgian National Fund for Scientific Research (NFWO) for financial support and for a travel grant to the University of Florida. A. Bogaerts and R. Gijbels also acknowledge financial support from the Federal Services for Scientific, Technical and Cultural Affairs (DWTC/SSTC) of the Prime Minister's Office through IUAP-III (Conv. 49). This research has been partially supported by DOE-DE-FG05-88ER13881 and DOE-DE-FG05-89ER14018.

References

[1] W.W. Harrison, Glow discharge mass spectrometry, in F. Adams, R. Gijbels and R. Van Grieken (Eds.), Inorganic Mass Spectrometry, Wiley, New York, 1988, Chapter 3.
[2] K.R. Hess and R.K. Marcus, Spectroscopy, 2 (1987).
[3] R.K. Marcus, Glow Discharge Spectroscopies, Plenum Press, New York, 1993.
[4] A. Bogaerts and R. Gijbels, J. Appl. Phys., 79 (1996) 1279.
[5] A. Bogaerts and R. Gijbels, Anal. Chem., 68 (1996) 2676.
[6] A. Bogaerts, M. van Straaten and R. Gijbels, Spectrochim. Acta Part B, 50 (1995) 179.
[7] A. Bogaerts, M. van Straaten and R. Gijbels, J. Appl. Phys., 77 (1995) 1868.
[8] A. Bogaerts, R. Gijbels and W.J. Goedheer, J. Appl. Phys., 78 (1995) 2233.
[9] A. Bogaerts and R. Gijbels, Phys. Rev., 52 (1995) 3743.
[10] A. Bogaerts and R. Gijbels, J. Appl. Phys., 78 (1995) 6427.
[11] A. Bogaerts, R. Gijbels and W.J. Goedheer, Anal. Chem., 68 (1996) 2296.
[12] A. Bogaerts and R. Gijbels, Fresenius' J. Anal. Chem., 355 (1996) 853.
[13] A.J. Stirling and W.D. Westwood, J. Phys. D: Appl. Phys., 4 (1971) 246.
[14] G. Absalan, C.L. Chakrabarti, J.C. Hutton, M.H. Back, C. Lazik and R.K. Marcus, J. Anal. At. Spectrom., 9 (1994) 45.
[15] K. Hoppstock and W.W. Harrison, Anal. Chem., 67 (1995) 3167.
[16] C. van Dijck, B.W. Smith and J.D. Winefordner, Spectrochim. Acta Part B, 37 (1982) 759.
[17] F.J. de Hoog, J.R. McNeil, G.J. Collins and K.B. Persson, J. Appl. Phys., 48 (1977) 3701.
[18] N.P. Ferreira and H.G.C. Human, Spectrochim. Acta Part B, 36 (1981) 215.
[19] E.M. van Veldhuizen and F.J. de Hoog, J. Phys. D: Appl. Phys., 17 (1984) 953.
[20] R.M. Allott, P.D. Miller, W.J. Jones and R.S. Mason, in G. Holland (Ed.), Recent Advances in Plasma Source Mass Spectrometry, K.D.M. International Scientific, Exeter, 1995, pp. 102–115.
[21] R.M. Allott, M. Kubinyl, A. Grofcsik, W.J. Jones and R.S. Mason, J. Chem. Soc. Faraday Trans., 91 (1995) 1297.
[22] C.H. Corliss and W.R. Bozman, Experimental Transition Probabilities for Spectral Lines of Seventy Elements, NBS Monograph 53, Washington DC, 1962.
[23] W. Schade and V. Helbig, Phys. Lett. A, 115 (1986) 39.
[24] N. Omenetto and J.D. Winefordner, Prog. Anal. At. Spectrosc., 2 (1979) 1.
[25] P. Ljungberg, D. Boudreau and O. Axner, Spectrochim. Acta Part B, 49 (1994) 1491.
[26] P. Ljungberg, D. Boudreau and O. Axner, Spectrochim. Acta (Electronica) Part B, 51 (1996) 413.
[27] J.D. Ingle and S.R. Crouch, Spectrochemical Analysis, Prentice Hall, New York, 1988.
[28] C.S. Rann, Spectrochim. Acta Part B, 23 (1968) 245.
[29] C.S. Rann, Spectrochim. Acta Part B, 23 (1968) 827.
[30] C.F. Bruce and P. Hannaford, Spectrochim. Acta Part B, 26 (1971) 207.
[31] C. Th.J. Alkemade, T. Hollander, W. Snelleman and P.J. Th. Zeegers, Metal Vapours in Flames, Pergamon Press, Oxford, 1982.
[32] H. Oechsner, Phys. Rev. B, 17 (1978) 1052.
[33] L. Vriens, Phys. Lett., 8 (1964) 260.

[34] A. Bogaerts, R.D. Guenard, B.W. Smith, J.D. Winefordner, W.W. Harrison and R. Gijbels, Spectrochim. Acta, Part B, 52 (1997) 219.
[35] L.A. Riseberg, W.F. Parks and L.D. Schearer, Phys. Rev. A, 8 (1973) 1962.
[36] A. Bogaerts and R. Gijbels, J. Anal. At. Spectrom., 11 (1996) 841.
[37] C.E. Moore, Atomic Energy Levels, Vols. I–III, Nat. Stand. Ref. Data Ser., Nat. Bur. Stand. (US), Washington DC, 1971.
[38] S. Johansson and U. Litzen, J. Phys. B, 11 (1978) L703.
[39] K. Danzmann and M. Koch, J. Phys. B, 14 (1981) 2989.
[40] P.B. Farnsworth and J.P. Walters, Spectrochim. Acta Part B, 37 (1982) 773.
[41] R.S. Hudson, L.L. Skrumeda and W. Whaling, J. Quant. Spectrosc. Radiat. Transfer, 38 (1987) 1.
[42] E.B.M. Steers and R.J. Fielding, J. Anal. Atom. Spectrom., 2 (1987) 239.
[43] E.B.M. Steers and F. Leis, Spectrochim. Acta Part B, 46 (1991) 527.
[44] E.B.M. Steers and A.P. Thorne, J. Anal. At. Spectrom., 8 (1993) 309.
[45] E.B.M. Steers, A.P. Thorne and Z. Weiss, 12th European Sectional Conference on the Atomic and Molecular Physics of Ionized Gases, Europhysics Conference Abstracts, 18E (1994) 65.
[46] K. Wagatsuma and K. Hirokawa, Spectrochim. Acta Part B, 51 (1996) 349.